Orbit Control of a Spacecraft around a Contact Binary Asteroid undergoing shape deformation

Jean-Baptiste H. Bouvier*, Koki Ho†
University of Illinois at Urbana-Champaign, Urbana, IL, 61801

Masatoshi Hirabayashi‡
Auburn University, Auburn, AL, 36849

This paper examines an orbit control problem for a spacecraft around a contact binary asteroid considering the dynamics of both the spacecraft and the asteroid itself. It is known that approximately 15% of the near-Earth asteroids are binary, and assuming a similar population spread as in the Kuiper Belt and among Trojan asteroids, the fraction of contact binaries is still significant : between 6 and 10% [1]. Most contact binary asteroids are constituted of an agglomeration of smaller boulders maintained together thanks to their internal gravity. Therefore, even a minor change in their mass repartition, like the landing of mining machines, can cause modification of the asteroid's structure including a landslide and a splitting. Particularly, separation of the asteroid into two parts is problematic in terms of orbit control, because of its consequences on the gravitational field of the asteroid. Traditional two-body orbital control methods cannot be applied to the missions to those asteroids because they do not consider the dynamic activities of the asteroids. This paper proposes and evaluates a control method to follow a predefined path under unknown states of the splitting and shape-changing binary asteroid.

I. Introduction

Recent emphasis on space explorations to asteroids has arisen in the last decades. Such explorations include collecting asteroidal materials for multiple purposes that widely range from scientific studies to engineering advance. Hayabusa, an asteroid sample return mission led by Japan Aerospace Exploration Agancy (JAXA), explored Itokawa, an asteroid orbing nearby the Earth, or a so-called Near-Earth Asteroid (NEA), and brought a surface material sample back to the Earth [2]. As of November 2018, JAXA-led Hayabusa2 [3] and NASA-led OSIRIS-REx [4, 5] are currently attempting to sample such material from target asteroids (162183) Ryugu and (101955) Bennu, respectively, with different technologies. To sample materials, the Hayabusa2 mission plans to land on Ryugu's surface, ignite a

*Master's Student, Aerospace Engineering, 306 Talbot Laboratory, MC-236, 104 South Wright Street, Urbana, Illinois 61801
†Assistant Professor, Aerospace Engineering, 306 Talbot Laboratory, MC-236, 104 South Wright Street, Urbana, Illinois 61801
‡Assistant Professor, Aerospace Engineering, Auburn University, 211 Davis Hall, Auburn, AL 36849

high-speed projectile to surface rocks, and collect fragmented materials inside a sampling system, which is called the sampler horn [3]. On the other hand, the OSIRIS-REx mission attempt to collect materials by controlling gas pressure inside the sampling system [5]. In addition, as a NASA/New Frontiers-level mission, CAESAR, one of two selected NASA/New Frontiers-level missions, is proposed to explore 67P/Churyumov-Gerasimenko, a comet whose orbit has been highly controlled by Jupiter, or a Jupiter Family Comet, and return a sample from this comet to the Earth (ref).

These asteroid exploration missions have shown potential expansion of our capabilities for proximal operations to the surface of asteroids. Complex operations in concepts and ongoing missions include direct interactions of spacecrafts with surface materials [6] or the structure of asteroids due to explosion [7]. Also, collecting a large amount of materials from asteroidal surfaces, or so-called asteroid mining [8], or deflecting potential hazardous asteroids by using kinetic impactors are part of applications and utilization of asteroids that require sophisticated technologies. NASA Double Asteroid Redirect Test (DART) is an ongoing mission, which is in Phase C, as of November 2018 [9]. In this mission, the DART spacecraft is designed to impact on a smaller secondary component of (65803) Didymos, a binary NEA but is also planned to release a CubeSat before the impact [9].

Such advanced proximal operations may change the gravitational configuration of a target asteroid. There are two reasons to address this issue. First, many small asteroids may be gravitational aggregates of small boulders, rocks, and regoliths, or so-called rubble piles as inferred from the spin conditions of observed asteroids [**?**] and from the derived bulk density and surface morphology of Itokawa [2] . Such asteroids do not have mechanical strengths, which are reportedly about 100 Pa [10, 11], implying that they might occasionally experience local and global landslides and internal deformation processes. These processes have been proposed to result from fast rotation and tidal effects. The second reason is that asteroids are irregularly shaped. Typically, their various shapes are categorized into four critical shapes: spheroidal, elongated, contact binary, and non-classified shapes [**?**]. Importantly, the shape is a critical parameter of the rotationally induced deformation mode [**?**].

Earlier work showed that when the shape of an asteroid changes, the gravity field of that asteroid also changes, leading to additional perturbation of the orbital motion. [**?**] demonstrated how the mutual motion of Didymos could change due to the shape deformation process of the primary whose spin period is reportedly 2.26 h, which may significantly control the magnitude of the centrifugal force, depending on the bulk density of this asteroid. They considered that at this fast rotation condition, once there was a kinetic energy input to the primary structure, the current shape configuration would become unstable and settle into a new shape configuration, causing shape deformation. They identified that such shape deformation significantly changes the gravity field, causing orbital perturbation.

We cast the following questions. How does the orbital motion of a spacecraft change when the asteroid structurally deforms during proximal operations? And, how robustly should control and navigation systems work to guide the spacecraft securely? This scenario may be likely to happen as proximal operations to asteroids become more complex. As mentioned above, some asteroids have fast rotation, which cause higher sensitivity to structural deformation as

centrifugal forces become dominant. In this case, shape deformation may occur due to small inputs that trigger large deformation [ref]. Also, when a spacecraft conducts impact operations, the crater formation processes cause critical deformation processes including compression beneath the surface and the formation of circular depression [ref]. Such deformation processes may induce a change in the gravity field [ref].

In this works, we consider a hypothetical situation in which our spacecraft is in proximal operations to a contact binary asteroid – an asteroid that consists of two lobes connecting with each other – that gradually deforms. Recent observations have shown that a contact binary configuration is in common in the solar system. For example, Itokawa and 1996 HW1 are involved in this asteroid type (Figure 1). Ground observations have shown that 15% of observed asteroids may have some features of contact binaries [Benner et al. 2015]. An example of a contact binary includes 1996 HW1 [???], Itokawa [Fujiwara et al., 2005], Castalia [Ostro et al....], and Toutatis [Ostro et al., ...] in near earth asteroids [NEAs] and Kleopatra [Ostro et al.] in the main belt asteroids (MBAs). For cometary nuclei, observations have revealed that about 70% of the observed objects at high resolution may be contact binaries. The nucleus of 67P/Churyumov-Gerasimenko is one of comets having a contact binary nucleus. A potential formation scenario of this object include a catastrophic disruption followed by a soft contact of two lobes [ref] and recontact after splitting of two lobes [ref]. If a contact binary asteroid reaches its critical limit of a structural condition, the neck part experiences inelastic deformation, causing the body to stretches along the minimum moment of inertia axis gradually [11]. To consider this condition, we introduce a simple model in which a contact binary is assumed to be a system that has two spherical bodies connecting with each other [ref].

We demonstrate a control and navigation technique for robustly achieving an expected trajectory. We make assumptions to implement an orbital control technique. First, the spacecraft possess sensors to measure its relative distance and velocity with respect to a considered contact binary asteroid. We propose a navigation technique that the spacecraft gives estimates of the asteroid's size, mass, and inertia during operation given measurement noise. To establish this method, we apply and Extended Kalman Filter (EKF)[12, 13]. A trajectory tracking algorithm developed by [14] is used to develop a technique for keeping the spacecraft in desired orbits. A proportional-integral-derivative (PID) controller is employed, followed by fine-tuning processes [15]. Thus, in our problem, the main system included a plant, a controller, and an estimator, which is based on Adaptive Control [16**?**].

II. Asteroid Modeling

A. Modeling of dynamics about a contact binary asteroid

In this work, we apply a simple asteroid model that mimics the gravity field of a contact binary asteroid [**?**]. This asteroid model consists of two spherical lobes that are connected with each other by a massless bar (Figure 1). Also, it initial rotates along the maximum moment of inertia axis with the spin rate, Ω. The masses of a larger lobe and a smaller

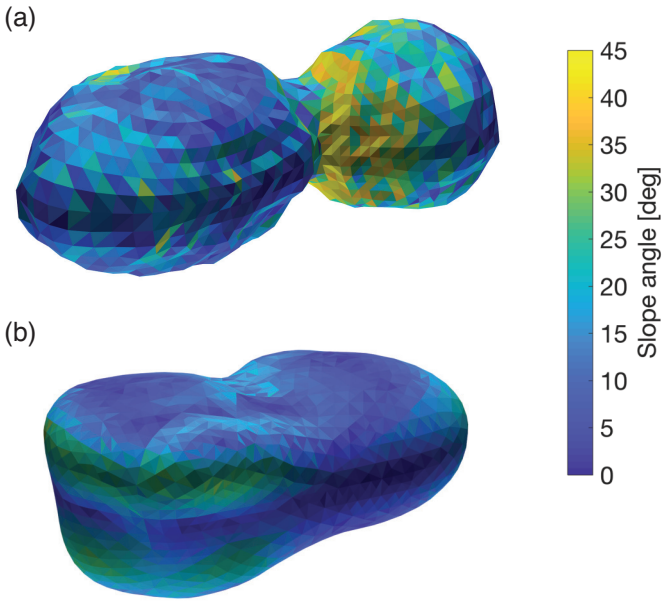

Fig. 1 Examples of contact binary asteroids. a. 1996 HW1 [?], and b. Castalia [?]. The contour shows the slope angle, which is an angle between the force direction (gravitational plus centrifugal forces) and an inward vector normal to the surface.

lobe are M_1 and M_2, respectively. Also, the radii of these parts are given as r_1 and r_2, respectively. The distance between the centers of mass of these lobes is defined as d. Also, the bulk density of these lobes is defined as ρ. Considering the coordinate frame rotating with this asteroid, we define potional space, $(x, y, z)^T$, where x is along the minimum moment of inertia axis, z is along the rotational axis, and y is in the orthogonal direction.

$$\ddot{x} - 2\Omega\dot{y} - \Omega^2 x = -\frac{Gm_1 d_1}{r_1^3} - \frac{Gm_2 d_2}{r_2^3}, \tag{1}$$

$$\ddot{y} + 2\Omega\dot{x} - \Omega^2 y = -\frac{Gm_1 y}{r_1^3} - \frac{Gm_2 y}{r_2^3}, \tag{2}$$

$$\ddot{z} = -\frac{Gm_1 z}{r_1^3} - \frac{Gm_2 z}{r_2^3}. \tag{3}$$

In contrast to the regular restricted three-body problem, Ω is a free parameter [**?**]. In a earlier study by [**?**], this parameter was considered to be constant. The present study, however, considers that Ω is no longer constant and varies as a function of time.

A spherical harmonics model [ref] may work at some level but may not be suitable for calculation of the gravity field inside the circumferential radius of the contact binary body, or known as XXX sphere. To this date, the most feasible model may be a polyhedron shape model that consists of a pile of tiles to generate the topography of an asteroid shape [Wenner, Wenner and Scheeres]. Many trajectory analyses about an irregularly shaped have been performed to better understand the complex orbital feature about such an object. Show some examples.

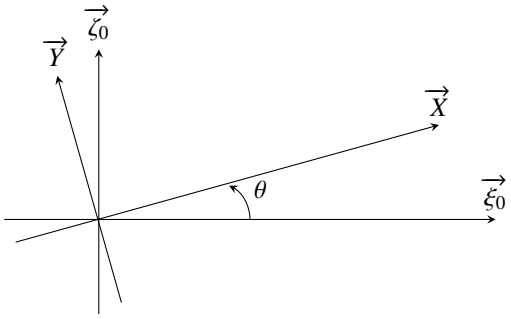

Fig. 2 Inertial and Rotating frames

Earlier work brought the following equation. Does an asteroid keep the original shape all the time? If not, how can a spacecraft dynamically behave? This question comes from the fact that many small asteroids are rubble piles, objects that are made by accumulations of small rocks and regoliths (the term of regolith was originally used by Sheomaker to describe small fragments on the Moon). In a violent environment in space, asteroids are always changing their configurations, causing shape deformation processes. Critical processes that cause shape deformation include high-velocity impacts, tidal effects, and fast rotations. All the processes usually connect with each other, providing unique surface color distribution of near-Earth asteroids (NEAs).

In the present work, we consider shape deformation processes due to fast rotation...

The contact binary asteroid considered for mining purposes is modeled as two spheres of same density ρ, and of radii r_1 and r_2 linked by α with $r_1 \geq r_2$.

$$r_1 = \alpha r_2 \qquad with\ \alpha \geq 1 \tag{4}$$

B. Two Body Problem Study

In relation to this work, after the lander cause the splitting of the asteroids, the spacecraft has no more direct impact on the asteroids' motion. Indeed, its mass is negligible with respect to that of the asteroids. Thus their motion can be derived by solving the Two Body Problem (2BP) equations. All the equations are written using the coordinates of the frame rotating with the asteroids. They both remain on the X-axis, and their motion can be characterized by the following parameters : d their splitting distance, Ω the angular velocity of the rotating frame, and m_1 and m_2 the masses of the two asteroids. Ω is defined as the time derivative of θ, the angle between the inertial reference frame and the rotating one. The equation of motion of the asteroids in the rotating frame can be written as :

$$\ddot{d} = d\Omega^2 - G\frac{(m_1 + m_2)}{d^2} \qquad with \quad G = 6.67408 \times 10^{-20}\ km^3 kg^{-1} s^{-2} \tag{5}$$

This equation gives the position of each asteroid. Indeed, by using the normalized constant mass parameter $\mu = \frac{m_2}{m_1+m_2}$ with $m_2 \leq m_1$, it is possible to ascertain the positions of each primary along the X-axis : $-\mu d$ for m_1 and

$(1-\mu)d$ for m_2.

Yet the angular velocity is also a function of the distance d. We first need the moment of inertia I of the asteroid. Considering two homogeneous spheres of radii r_1 and r_2, of masses m_1 and m_2 and separated with a distance d, the total inertia is:

$$I(d) = \frac{2}{5}\left(m_1 r_1^2 + m_2 r_2^2\right) + \frac{m_1 m_2}{m_1 + m_2} d^2 = I_{spheres} + m_1 \mu d^2 \tag{6}$$

Let us introduce $m_{tot} = m_1 + m_2$ the total mass of the asteroids, and the normalized inertia of the spheres: $I_n = \frac{I_{spheres}}{m_{tot}}$. Remarking that $m_1 = (1-\mu)m_{tot}$, we obtain:

$$\frac{I(d)}{m_{tot}} = I_n + \mu(1-\mu)d^2 \tag{7}$$

We normalize the inertia to have a variable of the same amplitude as the other components of the state vector. And now using the conservation of the angular momentum L, the angular velocity $\Omega(d)$ is linked to the splitting distance d :

$$L = I(d)\ \Omega(d) = I(d_0)\ \Omega(d_0) = I(d_0)\ \Omega_0 \tag{8}$$

Ω_0 being the initial rotating velocity of the asteroid. Then by normalizing this previous equation the angular velocity is reduced to $\Omega(d) = \Omega_0 \frac{I(d_0)}{m_{tot}} \frac{m_{tot}}{I(d)} = \Omega_0 \left(\frac{I_n + \mu(1-\mu)d_0^2}{I_n + \mu(1-\mu)d^2} \right)$. Which can now be introduced in eq. (5) to give a differential equation with only one variable d :

$$\ddot{d} = d\Omega_0^2 \left(\frac{I_n + \mu(1-\mu)d_0^2}{I_n + \mu(1-\mu)d^2} \right)^2 - \frac{G m_{tot}}{d^2} \tag{9}$$

As can be seen in the equation obtained from Newton's Second Law eq. (5), two opposite forces are applied on d : the gravitation that tends to bring the bodies closer and the centrifugal acceleration which has a repulsive action. Due to this opposition, an equilibrium exists and can be found by plugging $\ddot{d} = 0$ in eq. (5), and gives $\Omega_{eq}(R) = \sqrt{\frac{G(m_1+m_2)}{R^3}}$ with R the distance between the centers. When considering the initial situation with the contact binary asteroids, their initial angular velocity Ω_0 is arbitrary. The model adopted for the splitting operation assumes that the angular velocity is conserved. Then Ω_0 can be compared to $\Omega_{eq}(d_0)$ to predict the future motion of the asteroids.

- if $\Omega_{eq}(d_0) > \Omega_0$ the gravitation force is stronger than the centrifugal one, and thus the asteroids will not split, but stay in contact.
- if $\Omega_{eq}(d_0) < \Omega_0$ then the asteroids have enough energy to overcome the potential energy barrier and their splitting distance d will grow to infinity.

Only the second scenario is considered in this paper. This case brings restrictions on the period of the orbit of the spacecraft since once the smaller asteroid is out of the ellipse, the gravitational perturbations are too large for the craft to

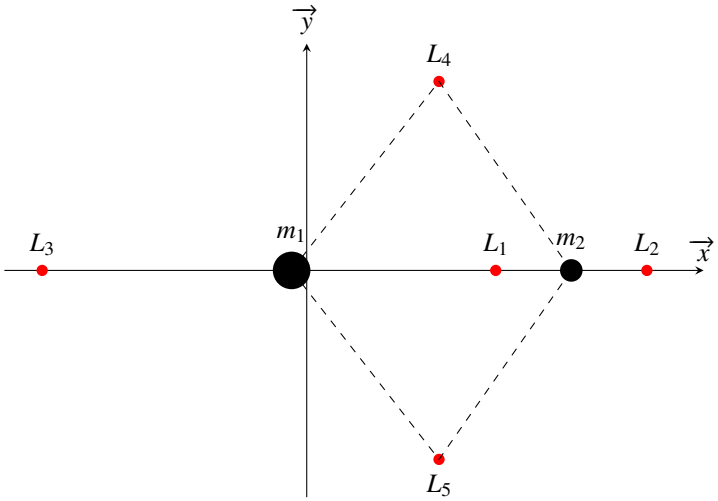

Fig. 3 Equilibrium points of the circular restricted 3 Body Problem

remain on the desired orbit.

C. Lagrange Points

To observe the asteroids several kinds of orbits can do the job. When considering the situation before splitting, so only one asteroid, the natural orbit choice would be circular or elliptical. This choice of orbit is considered in this paper. And even after the splitting, the control law aims at having the spacecraft remain on that two-bodies orbit.

Another approach would be to consider the situation after the splitting as reference for the orbit choice. Indeed, in the context of the 3BP other types of orbits become available. They are located around the gravitational equilibrium points of the system, which are called the Lagrange points and denoted L_i with $i \in \{1, 2, 3, 4, 5\}$.

For $i \in \{1, 2, 3\}$, L_i is dynamically unstable, thus orbits exist around these three collinear Lagrange points. Several different families of orbit exist among which are the HALO, Distant Retrograde Orbits (DRO), Planar Lyapunov orbits, Vertical Lyapunov,... However a necessary condition for these orbits to exist is that the Lagrange point considered is far enough from the asteroid. In fact in our case of a contact binary system, L_1 is initially inside the asteroid. Therefore an orbit around L_1 is impossible before the splitting. For L_2 and L_3 the answer is not as easy. Depending on the asteroids' mass ratio they can be inside or outside of the asteroids.

Plot distance L_2 to surface of asteroid as a function of α for different values of $\rho = 1.5 - 3$, same for L_3

Computing the position of the three collinear Lagrange points boils down to solving a quintic polynomial function, as described in the book John E Prussing [17].

$$(M_1 + M_2)X^5 + (3M_1 + 2M_2)X^4 + (3M_1 + M_2)X^3 - (3M_3 + M_2)X^2 - (2M_2 + 2M_3)X - (M_2 + M_3) = 0 \qquad (10)$$

M_1, M_2 and M_3 are masses assigned depending on the case considered. Since they are all positive, the six coefficients written in parenthesis in the previous equation are all positive. Thus the sign of each monomial is written. We can observe that there is only one change of sign, and the polynomials theory tells us that therefore there is only one positive root, which is the solution we are looking for. The solution X can be related to the three positions described in 3 : $X = \frac{x_3 - x_2}{x_2 - x_1}$ For instance if we want to determine the position of L_2, then the three bodies are ordered as m_1, m_2 and spacecraft at L_2, so the mass associated at each positions are : $M_1 = m_1$, $M_2 = m_2$ and $M_3 = 0$. Then we can solve eq. (10) for X. We are interested in $x_3 - x_2$, and we know the distance between primaries $x_2 - x_1$. L_2 being outside of the asteroid means $x_3 - x_2 > r_2$, i.e. $x_3 - x_2 = X(x_2 - x_1) = X(r_1 + r_2) = X(\alpha r_2 + r_2) = X(1 + \alpha)r_2 > r_2$ so we just want $X(1 + \alpha) > 1$but

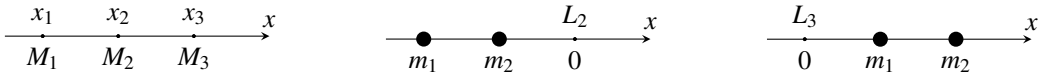

(a) General case **(b) Case : L2** **(c) case : L3**

Fig. 4 Different configurations to determine L_2 or L_3

III. Spacecraft Control Law

Considering a mission of exploration and landing on an asteroid, a pair lander/orbiter is the most general configuration. The orbiter collects data to learn about the asteroid structure and surface and thus prepares for the landing. In the eventuality of the asteroid splitting due to the lander, the orbiter has to adapt to this new situation by staying on orbit as long as possible. This scenario boils down to a station-keeping issue and thus a low-thrust propulsion system has been chosen over an impulsive one. Assuming as a first approach that only the asteroids and the spacecraft interact, the global calculation frame is the Restricted Three Body Problem. The Earth's and the Sun's gravitational attractions can be added later as perturbing forces. The attitude determination relies on position and velocity measurements of the spacecraft with respect to the asteroids which are then processed through an Extended Kalman Filter to compute the state. As for the thrust determination, a path following algorithm is implemented and tracks the desired elliptical orbit.

A. Implementation

1. Adaptive Control

The environment of the spacecraft is constantly evolving and only accessible through imperfect measurements. To model these uncertainties and account for unknown parameters (such as the asteroids masses, inertia,...), an adaptive control organization is necessary [18]. Adaptive control is usually divided into two broad categories : direct and indirect control. The latter category is the more natural process since unknown parameters are estimated and then used in the control law. Direct methods combine these two steps by calculating directly the control gains; the plant parameters are

not estimated. Even if these two approaches are philosophically different, they can be equivalent in some cases [19]. Two main reasons motivated the choice of an indirect method in this paper. First from a mission point of view, the orbiter has to collect information about the asteroid to prepare for the landing. Hence estimating the unknown plant parameters is already part of the mission, so these estimates can naturally be used to compute the control input. The other reason is that a Direct Control implementation requires a reference model which is not available in the case studied here. Indeed the first step of the Direct process is to take the difference between the state equation and the reference one to obtain the error $e = x - x_{ref}$. Then its time derivative $\dot{e}$ can be calculated, and used to build a candidate Lyapunov function V. Eventually, the stable control sought for will make $\dot{V} \leq 0$.

In the case considered in this paper, a reference model would be a trajectory to track, i.e. a list of positions, velocities and accelerations of the spacecraft around the asteroids. The positions are always available since the mission requirement is to follow a given geometrical path. However, obtaining velocity and acceleration can only be done through the whole orbit computation.

2. Orbit Computation

A coasting orbit is usually chosen as reference, in order to minimize the propellant consumption since even in that case, there will still be some thrust required for adjustments and station keeping. The method to compute a periodic coasting orbit is described in Koon et al. [20] :

- finding an initial position-velocity vector. The orbit being planar and symmetric with respect to the X-axis, a simple first guess vector would be : $X_0 = [x_0, 0, 0, 0, \dot{y}_0, 0]^t$. x_0 is directly linked to the radius of the orbit, so the only free parameter to determine is the initial velocity $\dot{y}_0$. An accurate first guess is $\dot{y}_0 = R_{orbit}\Omega_0 + \sqrt{\frac{G(m_1+m_2)}{R_{orbit}}}$, with R_{orbit} the radius of the desired orbit;
- propagating the trajectory until it hits the X-axis again. For the orbit to be periodic this final state must be of the following shape : $X_f = [x_f, 0, 0, 0, \dot{y}_f, 0]^t$. For a circular orbit $x_f = -x_0$ and $\dot{y}_f = -\dot{y}_0$. But usually $\dot{x}_f \neq 0$;
- updating the initial state X_0 to drive $\dot{x}_f$ to zero. These adjustments are made with a differential correction algorithm.
- propagating for a whole period once X_0 makes $|\dot{x}_f| \leq \epsilon$ with ϵ the desired precision.

The differential correction process is described in Chapter 4.2 of Koon et al. [20]. Assume we are starting around X_0 and we want to reach X_{goal} under the natural dynamics $\dot{X} = f(X)$. The process explains how to make small modifications of X_0. Let $\phi : (\tau, X_0) \rightarrow X(t)$ be the flow map, associating an initial state X_0 at t_0 to its value $X(\tau)$ after the natural propagation for a time τ. We want to perturb the initial state with δX_0 and see how the final state is modified. Let $\delta X(\tau)$ be the difference between the perturbed state and the original one, at the time τ, i.e. $\delta X(\tau) = \phi(\tau; X_0 + \delta X_0) - \phi(\tau; X_0)$. This expression can be developed with Taylor, and if only the leading term is conserved we obtain $\delta X(\tau) \simeq \frac{\partial \phi(\tau; X_0)}{\partial X_0} \delta X_0 = \Phi(\tau, t_0)\delta X_0$. Φ being the State Transition Matrix (STM).

Now we can apply this theory to our case. At the first iteration of the process we started from X_0 and reached X_f at the time t_f, while aiming at X_{goal}. Then $\delta X(t_f) = X_{goal} - X_f \simeq \Phi(t_f, t_0)\delta X_0$ with $\delta X_0 = X_{0,desired} - X_0$ being the only unknown and also the quantity we are looking for. Then to get $X_{0,desired}$ we just need to invert the STM. In our case the only component of X_0 that we want to modify is $\dot{y}_0$, so inverting the whole STM is a waste of time.

At each time step the primaries move further apart, so the previously computed orbit is not accurate anymore and must be recalculated. X_0 can then be reused as initial guess instead of restarting from scratch.

Because of the time-varying rotation velocity of the asteroids, the only periodic orbit in their rotating frame is the circular orbit. Therefore an elliptical orbit cannot be designed in the rotating frame using this previous method. The natural next step is then to try the inertial frame, because ellipses are periodic in that frame. However, that means recomputing the orbit at each time step with the primaries rotating inside. And their motion cause too much perturbations on the spacecraft trajectory to allow it to stay on an observation orbit close enough to the asteroids. Figure orbit here Since the coasting orbit cannot be computed, another option would be a low-thrust orbit that could be used as a reference. In that case the process at each time step would be :

- getting X_{ref} the reference state at the last time step;
- getting the geometrical path to follow during the time step;
- finding the thrust vector minimizing the error between the path and the propagation of X_{ref};
- using the whole Direct Adaptive process : calculate e, $\dot{e}$, V, $\dot{V}$, then u, the thrust vector for the actual state;

This method is too long, especially since the first steps could be applied directly to the actual state X, and then render the last step unnecessary.

Therefore the overall implementation follows an Indirect Adaptive Control scheme composed of three different blocks. The controller computes the thrust vector based on the reference path to follow and the current state, its precise functioning is described in subsection III.D. The plant propagates the state a time step ahead using the Three Body Equations detailed in III.B. The estimator refines the accuracy of the state using measurements as explained in subsection III.C

The scheme described previously corresponds to a Self-Tuning Controller (STC) as defined in Lavretsky [16]. The main issue of this scheme is that its bedrock is the Certainty Equivalence Principle : the control u is computed from the estimates as if they were true. This happens because Controller and Estimator are two different blocks as can be seen on Figure 5 .

B. Restricted Three Body Problem Equations

In the usual studies of the Three Body Problem (3BP) the primaries are one celestial body and one of its satellite, the third body being the spacecraft whose trajectory is to be described. The most commonly studied 3BP is the Circular Restricted Three Body Problem (CR3BP), in which the smaller primary has a circular orbit around the other body.

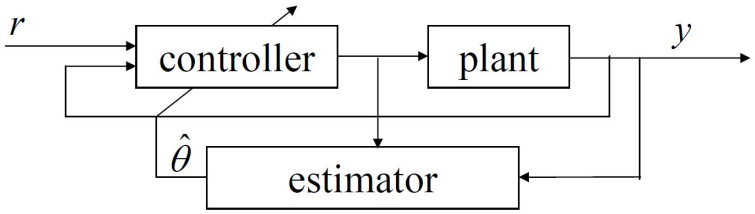

Fig. 5 Self-Tuning Controller (from Lavretsky [16])

Almost all the literature dealing with a more global case than this simplified one dates back to the 1960s Szebehely [21]. The study of a contact binary asteroid that starts splitting does not fit in the CR3BP case, because the distance between these primaries is not constant and the rotation of the whole system is also time-varying. Thus, none of the usual normalization of the CR3BP can be used. For this reason all the calculations are run with the International System units.

The frame used for the calculations is the rotating frame with a time-varying rotation velocity Ω that brings all three rotating acceleration terms : the centrifugal, Euler and Coriolis forces.

The state vector is a 15-components vector $\mathbf{X}$ containing the six usual coordinates of the spacecraft plus the distance between the primaries d and their splitting velocity $\dot{d}$, accompanied by θ the angle between the inertial reference frame and the rotating one. The 6 following components are constant parameters to be estimated : the masses of the asteroids : m_1 and m_2, their moment of inertia : I_1 and I_2,

$$\mathbf{X} = [x, y, z, d, \dot{x}, \dot{y}, \dot{z}, \dot{d}, \theta, m_1, m_2, I_1, I_2, \Omega_0, d_0]^t \tag{11}$$

Since the relevant frame is rotating with respect to the inertial one, the forces considered are the rotating acceleration terms, the control thrust and the gravitational attraction of the two primaries on the spacecraft. The latter is too light to affect the asteroids' motion.

$$m\vec{d} = \overrightarrow{F_{G1}} + \overrightarrow{F_{G2}} - 2m\vec{\Omega} \times \vec{v} - m\vec{\Omega} \times (\vec{\Omega} \times \vec{r}) - m\frac{d\vec{\Omega}}{dt} \times \vec{r} + \vec{u} \tag{12}$$

After some calculations, eq. (5) and eq. (12) can be gathered using the 15-components vector formulation :

$$\dot{\mathbf{X}} = \mathbf{f}(\mathbf{X}, \mathbf{u}) = \begin{bmatrix} \dot{x} \\ \dot{y} \\ \dot{z} \\ \dot{d} \\ -G\frac{m_1 d_1}{r_1^3} - G\frac{m_2 d_2}{r_2^3} + \frac{u_x}{m} + x\Omega^2 + 2\dot{y}\Omega + y\dot{\Omega} \\ -G\frac{m_1 y}{r_1^3} - G\frac{m_2 y}{r_2^3} + \frac{u_y}{m} + y\Omega^2 - 2\dot{x}\Omega - x\dot{\Omega} \\ -G\frac{m_1 z}{r_1^3} - G\frac{m_2 z}{r_2^3} + \frac{u_z}{m} \\ d\Omega^2 - G\frac{(m_1+m_2)}{d^2} \\ \Omega \\ 0 \\ 0 \\ 0 \\ 0 \\ 0 \\ 0 \end{bmatrix} \quad with \quad \Omega(d) = \sqrt{G\frac{(m_1+m_2)}{d_0^3}}\left(\frac{K+d_0^2}{K+d^2}\right)$$

with $d_1 = x + \mu d$ and $d_2 = x - (1-\mu)d$ $r_1 = \sqrt{d_1^2 + y^2 + z^2}$ and $r_2 = \sqrt{d_2^2 + y^2 + z^2}$

The Jacobian of $\mathbf{f}$ can then be calculated :

$$\mathbf{F} = \frac{\partial \mathbf{f}}{\partial \mathbf{X}} = \left[\begin{array}{c|c|c|c} 0_{4\times4} & I_{4\times4} & 0_{4\times1} & 0_{4\times6} \\ \hline dF_{4\times4} & \Omega_{4\times4} & 0_{4\times1} & dCST_{4\times6} \\ \hline 0_{1\times4} & 0_{1\times4} & 0_{1\times1} & 0_{1\times6} \\ \hline 0_{6\times4} & 0_{6\times4} & 0_{6\times1} & 0_{6\times6} \end{array}\right]$$

All the details are in Appendix A V. The shape of the top left 8×8 sub-matrix of $\mathbf{F}$ is very similar to the one used in the CR3BP to propagate the State Transition Matrix (STM); it is serving the same purpose here. The addition of the constants results in the addition of the six last columns and rows which are almost all empty.

C. Extended Kalman Filter

Since the spacecraft can only get access to its state through noisy measurements, an algorithm to refine those values and acquire accurate data is required. To fulfill this task an Extended Kalman Filter (EKF) with discrete time measurements has been implemented.

With the same notations as preceding X is the estimated state and Y the actual state, f is the state transition function, F its Jacobian, Z the observation and u the thrust. The other matrices come from the EKF and are respectively : R the covariance matrix of the measuring noise $V(t)$, Q the covariance matrix of the process noise $W(t)$, h the observation

function and H its Jacobian, G the gain matrix, P is the prediction error and I the identity matrix of the appropriate size.

MODEL	*PREDICT*	*UPDATE*
$\dot{Y}(t) = f\Big(Y(t),\ u(t)\Big) + W(t)$	$\dot{X}(t) = f\Big(X(t),\ u(t)\Big)$	$G = PH^t(HPH^t + R)^{-1}$
$Z = h(Y) + V(t)$	$\dot{P}(t) = F(t)P(t) + P(t)F^t(t) + Q$	$X = X + G(Z - h(X))$
		$P = (I - GH)P$

The observation Z is the information received by the spacecraft. Z is composed of two 6-components position-velocity vectors between the spacecraft and both asteroids. The sensors measure distance and speed in the inertial frame based on fixed stars. For simplicity's sake, it has been assumed that the frame of the asteroids rotates around the Z-axis of the inertial frame. This rotations is parametrized by the angle θ and its time derivative $\frac{d\theta}{dt} = \Omega(t)$. So the observation function transforms a 15-components rotating vector into two 6-components inertial vectors :

$$\mathbf{h}(\mathbf{X}) = \left[\begin{array}{c} cos(\theta)(x + \mu d) - sin(\theta)y \\ sin(\theta)(x + \mu d) + cos(\theta)y \\ z \\ -\Omega\big(sin(\theta)(x + \mu d) + cos(\theta)y\big) + cos(\theta)(\dot{x} + \mu\dot{d}) - sin(\theta)\dot{y} \\ \Omega\big(cos(\theta)(x + \mu d) - sin(\theta)y\big) + sin(\theta)(\dot{x} + \mu\dot{d}) + cos(\theta)\dot{y} \\ \dot{z} \\ \hline cos(\theta)(x - (1-\mu)d) - sin(\theta)y \\ sin(\theta)(x - (1-\mu)d) + cos(\theta)y \\ z \\ -\Omega\big(sin(\theta)(x - (1-\mu)d) + cos(\theta)y\big) + cos(\theta)(\dot{x} - (1-\mu)\dot{d}) - sin(\theta)\dot{y} \\ \Omega\big(cos(\theta)(x - (1-\mu)d) - sin(\theta)y\big) + cos(\theta)(\dot{x} - (1-\mu)\dot{d}) + cos(\theta)\dot{y} \\ \dot{z} \end{array}\right]$$

The observation has to be built from the state to follow the EKF process, and that is the reason of the presence of θ in the state vector. The detailed calculations of the Jacobian $H = \frac{\partial h}{\partial X}$ can be found in Appendix B section V.

Concerning the prediction error matrix P, several improvements have been implemented following the advice from Schneider and Georgakis [13]. First comes the choice of the initial value P_0. The prediction matrix contains values between zero and one, based on the confidence on the accuracy of the estimates; 0 being for a perfect estimate and 1 for a poor estimation. The best initialization is to take $P_0 = (X_0 - Y_0)^T \cdot (X_0 - Y_0)$ because it directly quantifies the precision of the estimate. However, the actual intial state Y_0 must be available, which is not the case here. A simple option would be to initialize P_0 as a matrix full of ones, then no over-confidence is given to any estimate. Yet assigning the worst initialization is not a good idea, since some information is available concerning the initial state. Indeed, the approximate size of the zone around the estimate where the true value lies is usually known. The initial state estimate

X_0 is built from the true one using $X_0 = D \cdot Y_0$, with D a diagonal matrix which terms follow a normal distribution of average one and of standard deviation $\sigma = 0.07$. It is reasonable to assume this σ known since it characterizes the previously mentioned size of the zone. And then $P_0 = (2\sigma X_0)^T \cdot (2\sigma X_0)$.
The second improvement is a more robust update equation for P using the Joseph stabilized version :
$P = (I - GH)P(I - GH)^T + GRG^T$

D. Controller

The controller is the part of the process that designs the control input, for the current position to track a certain reference described in the mission requirements. In this paper the spacecraft aims at orbiting elliptically around the asteroids. The controller can be designed along two main philosophies : Path Following or Trajectory Tracking.

A path is a list of positions, while a trajectory also has a timing law associated, i.e. a velocity and acceleration at each position. Yet having both of them available on the desired trajectory is not always the case. Moreover for a specific mission or due to a very unusual asteroid shape, the orbit may need to be specifically designed for this case and to be more complicated than a circle or an ellipse. In such a case, the propagation of the desired orbit can be a lot more difficult, as detailed in section III.A, especially to obtain in real-time the desired acceleration and velocity at a certain position.

Thus the solution is to implement a Path Following strategy, using a slight variation of the method developed in [22]. The usual method is to add an extra control parameter in order to describe the timing law which parametrizes the position to track on the desired path, transforming path following into trajectory tracking. And then at each time step an optimization problem must be solved to find the best thrust and timing law for the next step. In a Trajectory Tracking context a PID controller would be used to stabilize the trajectory close to the desired path. Yet in the Path Following case the velocity and acceleration on the path are not available so we cannot implement a Feedback Linearization algorithm with a PID controller. Instead, the thrust computation algorithm has access to a longer time horizon, to be able to anticipate and prevent divergences. This anticipation helps preventing overshoot and oscillations which usually happen when trying to minimize the distance to a path when looking only one time step ahead.

The timing-law is also an extra parameter to optimize but the insights about its value are difficult to acquire. Thus a simpler method has been implemented, the position to track is just the point on the desired path that is the closest to the current position.

At each time step the best thrust to apply to the spacecraft is calculated. For a predetermined thrust, the trajectory is propagated for a number PH of time steps δt, PH being the Prediction Horizon. And then the integral error of this trajectory with respect to the desired path is calculated following the method described in [23]. This error is considered as a cost to minimize and this optimization problem is to be solved at each time step in order to determine the best thrust vector.

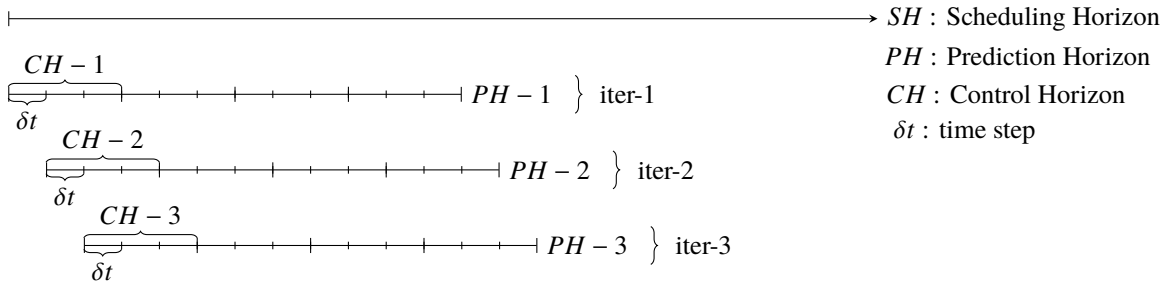

Fig. 6 Rolling Horizon with $N = 4$ and $H = 3$

The minimization problem to solve is finding the thrust vector u in order to minimize the error. u is bounded with u_{inf} and u_{sup}, which are characteristics of the thrust system.

$$\min_{\forall t, u_{inf} \leq u(t) \leq u_{sup}} \int_{t_0}^{t_0+PH} ||X\big(t, u(t)\big) - X_{ref}(t)||\, dt \tag{13}$$

The implementation being not continuous, the thrust is constant per time step, so eq. (13) has to be modified. A rolling horizon method is implemented with four different time scales, as described in fig. 6.

- The Scheduling Horizon SH is the total time range of the mission;
- The Prediction Horizon PH is subdivided into N Control Horizons : $PH = N \times CH$. At each time step the state is propagated over PH for the system to anticipate and provide an appropriate answer;
- Over the Control Horizon CH, the thrust is considered constant. It can be divided into H time steps δt because the thrust does not vary too much over just one time step. So $CH = H \times \delta t$. The thrust will actually change at the next time step, but this process allows to look further ahead for almost the same computation time;
- The time step δt is the smallest time scale, it corresponds to the step of the iterations of the state propagation;

To sum up, there are two design parameters for this rolling horizon scheme : the integers N and H. Their values will be optimized in the section IV. We can now update eq. (13) with the rolling horizon to finally obtain eq. (14)

$$\min_{\substack{u_{inf} \leq u_1 \leq u_{sup} \\ \vdots \\ u_{inf} \leq u_N \leq u_{sup}}} \sum_{k=1}^{N} \int_{t_0+(k-1)CH}^{t_0+kCH} ||X(t, u_k) - X_{ref}(t)||\, dt \tag{14}$$

In the current implementation only the elliptical and circular orbits cases have been considered, leading to a specific algorithm to calculate the distance between the spacecraft and the closest point on the path. But more general algorithm exist [24] and allow any type of orbit to be followed.

A common issue arising from this algorithm is that the direction in which to follow the path is not prescribed and thus the minimization can also lead to an abrupt turn-around. To prevent this a simple sign check of the cross product between the position vectors and the beginning and end of the time Horizon can be performed, and a higher cost given

to the non-wanted direction of propagation.

IV. Results

A. Controller Optimization

The test case uses the values gathered in the Table 1 The asteroid 4179 Toutatis [25] has been chosen, because orbiting close to the Earth with a low inclination and big enough to be considered for a mission objective like the Chinese flyby in December 2012. The Spacecraft model is close to the orbiter Rosetta that performed a similar mission. The orbit has been chosen big enough for the spacecraft to complete a whole orbit after the splitting while the final distance between the asteroids is comparable to the orbit size.

Table 1 Value of the main parameters for the test case

Asteroid	Value	Orbit	Value	Spacecraft	Value	Other	Value
r_1	1.5 km	Semi major axis	75 km	m_{SC}	3×10^3 kg	T_{step}	2 sec
α	2.5	Eccentricity	0.5	Max thrust	1 N	Horizon	20 sec
ρ	2000 $kg\,m^{-3}$					d_{CUT}	10 km
Ω_0	$1.3517 \times 10^{-5} sec$						

r_1 and α are defined in equation 4. ρ is the density of the asteroids. $\dot{d}_0$ is the initial splitting velocity of the asteroids. Ω_0 is the initial rotating velocity of the asteroids. T_{step} is the time step for the calculations, it can be compared to the time necessary for the Spacecraft to complete a total revolution : $T \simeq 2 \times 10^3$ sec.

The first step of the process is to prove that a control law is actually needed, because the natural dynamics of the spacecraft would not maintain it on orbit around the splitting asteroids. For Toutatis when no thrust is applied the spacecraft flies away as can be seen in Figure 7a.

For this test case the actual and estimated orbits are both really close to the desired ellipse as can be seen on Figure 7b.

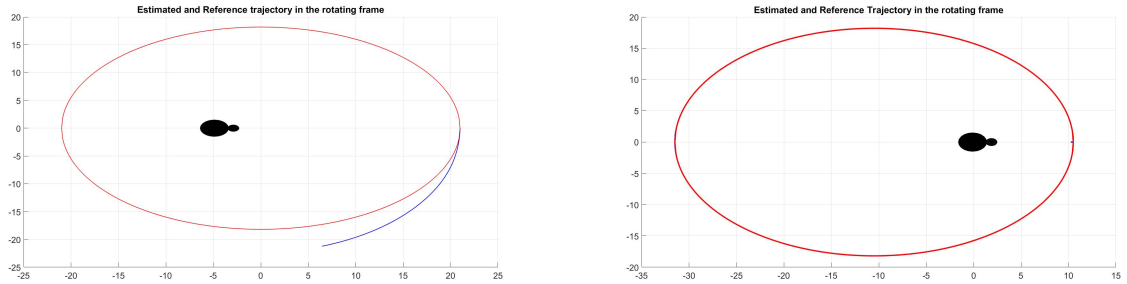

(a) No thrust **(b) Controlled thrust**

Fig. 7 Orbit around Toutatis in the rotating frame

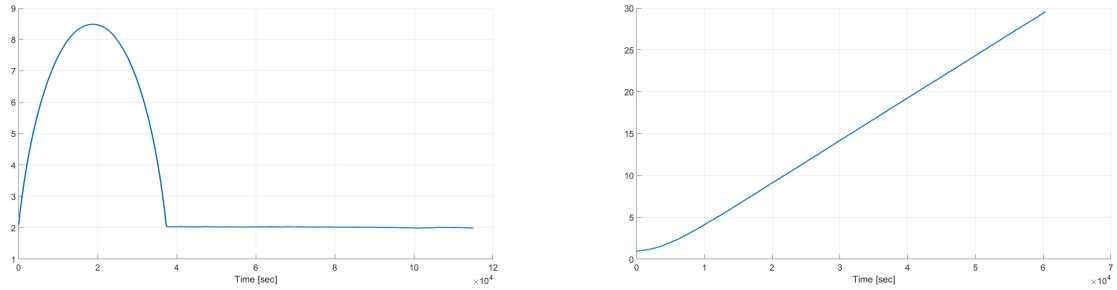

(a) Toutatis **(b) Castalia**

Fig. 8 Evolution of the distance between primaries

The initialization of the estimated state is noisy and completely out of the path, but the EKF corrects it in a few iterations. Yet for the Toutatis asteroid the initial rotating velocity is too small compared to the equilibrium rotating velocity : $\Omega_0 < \Omega_{eq}$, and then the two asteroids parts will split of a dozen kilometers before collapsing back together. The same would happen for 1996 HW1 and 25143 Itokawa. Only 4769 Castalia has comparable values of Ω_0 and Ω_{eq}. Indeed Ω_0 is fixed, given by the observations data, but Ω_{eq} depends on the model and the size of the spheres to represent this contact binary asteroids. For a choice of $r_1 = 0.65\ km$, $r_2 = 0.3\ km$ and $\rho = 1.8\ g/cm^3$, the values of the rotating velocities are : $\Omega_0 = 4.36 \times 10^{-4}\ rad/s > \Omega_{eq} = 4.2 \times 10^{-4}\ rad/s$. So the primaries splitting distance can be compared in fig. 8

And the computed orbit in the case of the asteroid 4769 Castalia is in Figure fig. 9

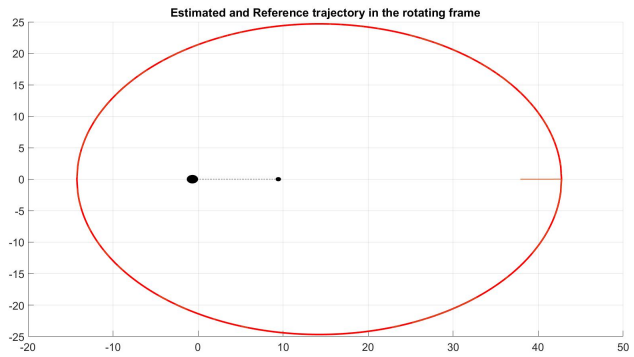

Fig. 9 Orbit around the asteroids in their rotating frame

B. Algorithm parameters choice

Two parameters of the algorithm must be chosen by the user : the Horizon size H defining the number of time steps to look ahead when determining the new thrust. If H is too small then the controller cannot anticipate trajectory modifications and then overshoot phenomenon take place, leading to numerous unwanted oscillations as can be seen in Figure fig. 10

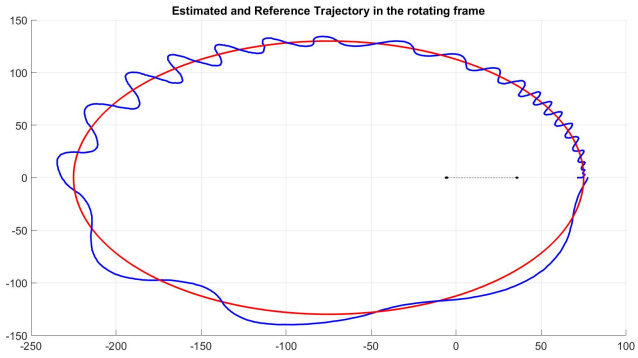

Fig. 10 Orbit for Horizon H = 1

On the other hand if H is too big, the calculations are obviously slower because the propagation must be computed over a longer time span, but the results are also worse as can be seen in Figure 11. The best value for H seems to be 5.

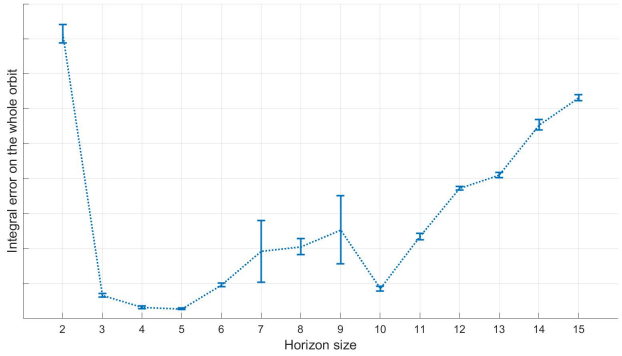

Fig. 11 Integral of the position error as a function of the Horizon H

Indeed, the thrust is constant over the whole horizon, so the correction and convergence back on path are slower. This choice of constant thrust is dictated by the algorithm run time, that is drastically cut down when asked to perform the minimization over only 3-components of thrust, instead of $3 \times H$ if the thrust is allowed to change at each time step within the horizon. The results of this comparison can be found in Table 2. The horizon value was fixed at $H = 8$, and 20 repetitions were performed.

Table 2 Comparison between constant and variable thrust for optimization

	Constant	Variable
Integral Error	km	km
Run time	sec	sec

The accuracy improvement are not significant but the computation time increased by a factor ??. Therefore the method employed will still use a constant thrust over the horizon.

However, for some cases an horizon of only 5 or 8 time steps is not enough compared to the thousand time steps required for the whole orbit. The algorithm cannot anticipate enough and that can cause a divergence from the desired orbit. To improve its anticipation skills a longer horizon is needed. To do so without increasing too much the computation time, the solution is to keep the value of H but consider several horizons at a time. Let call N this number of horizons. So the optimizer has to determine N thrust vectors, and the algorithm can look $N \times H$ time steps ahead with a constant thrust over each horizon.

C. Monte-Carlo simulations

To test the robustness of the implementation, several Monte-Carlo simulations have been performed. The parameters and their upper and lower bounds are described in the Table 3

Table 3 Bounds of the parameters tested

Parameter	Lower bound	Upper bound
r_1	0.2 km	10 km
α	1	10
ρ	1000 $kg\,m^{-3}$	3000 $kg\,m^{-3}$
sma	5 d_0	20 d_0
ecc	0	0.9
$\dot{d}_0$	10^{-3} $m\,s^{-1}$	2 $m\,s^{-1}$
Ω_0	Ω_{eq}	$4\,\Omega_{eq}$

Table 4 Monte Carlo parameters

Parameter	Value
Number of iterations	1000
d_{CUT}	5% sma

The semi major axis of the ellipse sma is defined as a multiple of the initial distance between the asteroids center $d_0 = r_1 + r_2 = r_1\left(1 + \frac{1}{\alpha}\right)$. Ω_0 is chosen as a multiple of the equilibrium value Ω_{eq} for which the asteroids would collapse back together if they had no initial velocity. These last two parameters are of primary importance for the asteroids trajectory. If chosen too big the primaries will split too quickly and when their distance becomes comparable to the semi major axis of the orbit then the station keeping will become too expensive.

For each simulation, a random value for the seven parameters is chosen among these bounds, and then the orbit is propagated for a complete revolution. If at some point during the propagation the position error of the spacecraft with respect to the desired trajectory is larger than 5% of the semi major axis of the orbit, then the propagation is stopped and an infinity value is assigned to the cost.

D. Shape changing asteroids

The splitting process of the asteroids can be rough and trigger modifications of the parts. For instance a landslide would result in a shape change and thus in a modification of the inertia of the asteroid. A change in mass can also be tackled because the splitting can result into two main asteroid bodies plus certainly a multitude of smaller parts sent flying away. To implement these modifications the white noise applied to our equation of motions, namely the process

noise as described in the EKF then become a non-zero mean noise. Due to the scarcity of data concerning asteroid splitting, the value chosen for the average of the mass change is the mass loss rate of the comet HALE-BOPP [26]. It has a mass $M \simeq 5 \times 10^{11}\ kg$ and a mass loss rate $\dot{M} \simeq 10^{6}\ kg/s$. So the equivalent mass loss rate scaled to the asteroid of mass m_1 is $\dot{m}_1 = m_1 \frac{\dot{M}}{M} \simeq 2 \times 10^{-6} \times m_1 kg/s$.

For the moment of inertia, the mean value is the one required to go from a ball to an ellipsoid with a radius twice longer in the time needed for the spacecraft to perform a whole orbit. So along the principal axis the inertia goes from $I_0 = \frac{2}{5}mr^2$ to $I_f = \frac{8}{5}mr^2 = 4I_0$ in a time T. Assuming a linear growth, $I_f = I(T) = I_0 + T\dot{I} = 4I_0$. Then $\dot{I} = \frac{3I_0}{T}$.

Even with these perturbations the path following algorithm is still able to track the orbit and the estimated values of the mass and inertia also follow the trend of the actual values as can be seen in Figure 12.

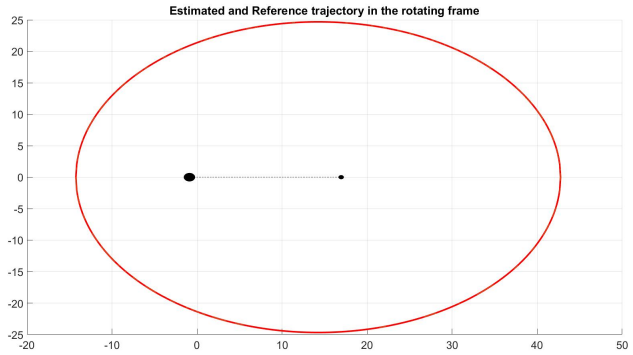

Fig. 12 Orbit around the asteroids in their rotating frame

V. Conclusion

The orbit control of a spacecraft around a splitting binary asteroid has been studied

Appendix A : details of the Jacobian F

$$
\mathbf{F} = \frac{\partial \mathbf{f}}{\partial \mathbf{X}} = \left[\begin{array}{cccc|cccc|c|cccccc}
0 & 0 & 0 & 0 & 1 & 0 & 0 & 0 & 0 & 0 & 0 & 0 & 0 & 0 & 0 \\
0 & 0 & 0 & 0 & 0 & 1 & 0 & 0 & 0 & 0 & 0 & 0 & 0 & 0 & 0 \\
0 & 0 & 0 & 0 & 0 & 0 & 1 & 0 & 0 & 0 & 0 & 0 & 0 & 0 & 0 \\
0 & 0 & 0 & 0 & 0 & 0 & 0 & 1 & 0 & 0 & 0 & 0 & 0 & 0 & 0 \\
\hline
\frac{\partial f_5}{\partial x} & \frac{\partial f_5}{\partial y} & \frac{\partial f_5}{\partial z} & \frac{\partial f_5}{\partial d} & 0 & 2\Omega & 0 & \frac{\partial f_5}{\partial \dot{d}} & 0 & \frac{\partial f_5}{\partial m_1} & \frac{\partial f_5}{\partial m_2} & \frac{\partial f_5}{\partial I_1} & \frac{\partial f_5}{\partial I_2} & \frac{\partial f_5}{\partial \Omega_0} & \frac{\partial f_5}{\partial d_0} \\
\frac{\partial f_6}{\partial x} & \frac{\partial f_6}{\partial y} & \frac{\partial f_6}{\partial z} & \frac{\partial f_6}{\partial d} & -2\Omega & 0 & 0 & \frac{\partial f_6}{\partial \dot{d}} & 0 & \frac{\partial f_6}{\partial m_1} & \frac{\partial f_6}{\partial m_2} & \frac{\partial f_6}{\partial I_1} & \frac{\partial f_6}{\partial I_2} & \frac{\partial f_6}{\partial \Omega_0} & \frac{\partial f_6}{\partial d_0} \\
\frac{\partial f_7}{\partial x} & \frac{\partial f_7}{\partial y} & \frac{\partial f_7}{\partial z} & \frac{\partial f_7}{\partial d} & 0 & 0 & 0 & 0 & 0 & \frac{\partial f_7}{\partial m_1} & \frac{\partial f_7}{\partial m_2} & 0 & 0 & 0 & 0 \\
0 & 0 & 0 & \frac{\partial f_8}{\partial d} & 0 & 0 & 0 & 0 & 0 & \frac{\partial f_8}{\partial m_1} & \frac{\partial f_8}{\partial m_2} & \frac{\partial f_8}{\partial I_1} & \frac{\partial f_8}{\partial I_2} & \frac{\partial f_8}{\partial \Omega_0} & \frac{\partial f_8}{\partial d_0} \\
\hline
0 & 0 & 0 & -\frac{2d\Omega}{K+d^2} & 0 & 0 & 0 & 0 & 0 & \frac{\partial \Omega}{\partial m_1} & \frac{\partial \Omega}{\partial m_2} & \frac{\partial \Omega}{\partial I_1} & \frac{\partial \Omega}{\partial I_2} & \frac{\partial \Omega}{\partial \Omega_0} & \frac{\partial \Omega}{\partial d_0} \\
\hline
0 & 0 & 0 & 0 & 0 & 0 & 0 & 0 & 0 & 0 & 0 & 0 & 0 & 0 & 0 \\
0 & 0 & 0 & 0 & 0 & 0 & 0 & 0 & 0 & 0 & 0 & 0 & 0 & 0 & 0 \\
0 & 0 & 0 & 0 & 0 & 0 & 0 & 0 & 0 & 0 & 0 & 0 & 0 & 0 & 0 \\
0 & 0 & 0 & 0 & 0 & 0 & 0 & 0 & 0 & 0 & 0 & 0 & 0 & 0 & 0 \\
0 & 0 & 0 & 0 & 0 & 0 & 0 & 0 & 0 & 0 & 0 & 0 & 0 & 0 & 0 \\
0 & 0 & 0 & 0 & 0 & 0 & 0 & 0 & 0 & 0 & 0 & 0 & 0 & 0 & 0
\end{array}\right]
$$

$$K = \frac{\frac{2}{5}\left(m_1 r_1^2 + m_2 r_2^2\right)}{\frac{m_1 m_2}{m_1 + m_2}} \quad \textit{inertial constant}$$

$$d_0 = r_1 + r_2$$

$$\Omega(d) = \sqrt{G \frac{(m_1 + m_2)}{d_0^3} \left(\frac{K + d_0^2}{K + d^2}\right)}$$

$$\dot{\Omega} = -\frac{2d\dot{d}\Omega}{K + d^2}$$

Appendix B : details of the Jacobian H

$$
\mathbf{H} = \frac{\partial \mathbf{h}}{\partial \mathbf{X}} = \left[\begin{array}{cccc|cccc|ccccccc}
cos(\theta) & -sin(\theta) & 0 & \mu cos(\theta) & 0 & 0 & 0 & 0 & \frac{\partial h_1}{\partial \theta} & \frac{\partial h_1}{\partial m_1} & \frac{\partial h_1}{\partial m_2} & \frac{\partial h_1}{\partial I_1} & \frac{\partial h_1}{\partial I_2} & \frac{\partial h_1}{\partial \Omega_0} & \frac{\partial h_1}{\partial d_0} \\
sin(\theta) & cos(\theta) & 0 & \mu sin(\theta) & 0 & 0 & 0 & 0 & \frac{\partial h_2}{\partial \theta} & \frac{\partial h_2}{\partial m_1} & \frac{\partial h_2}{\partial m_2} & \frac{\partial h_2}{\partial I_1} & \frac{\partial h_2}{\partial I_2} & \frac{\partial h_2}{\partial \Omega_0} & \frac{\partial h_2}{\partial d_0} \\
0 & 0 & 1 & 0 & 0 & 0 & 0 & 0 & 0 & 0 & 0 & 0 & 0 & 0 & 0 \\
-\Omega sin(\theta) & -\Omega cos(\theta) & 0 & \frac{\partial h_4}{\partial d} & cos(\theta) & -sin(\theta) & 0 & \mu cos(\theta) & \frac{\partial h_4}{\partial \theta} & \frac{\partial h_4}{\partial m_1} & \frac{\partial h_4}{\partial m_2} & \frac{\partial h_4}{\partial I_1} & \frac{\partial h_4}{\partial I_2} & \frac{\partial h_4}{\partial \Omega_0} & \frac{\partial h_4}{\partial d_0} \\
\Omega cos(\theta) & -\Omega sin(\theta) & 0 & \frac{\partial h_5}{\partial d} & sin(\theta) & cos(\theta) & 0 & \mu sin(\theta) & \frac{\partial h_5}{\partial \theta} & \frac{\partial h_5}{\partial m_1} & \frac{\partial h_5}{\partial m_2} & \frac{\partial h_5}{\partial I_1} & \frac{\partial h_5}{\partial I_2} & \frac{\partial h_5}{\partial \Omega_0} & \frac{\partial h_5}{\partial d_0} \\
0 & 0 & 0 & 0 & 0 & 0 & 1 & 0 & 0 & 0 & 0 & 0 & 0 & 0 & 0 \\
\hline
cos(\theta) & -sin(\theta) & 0 & -(1-\mu)cos(\theta) & 0 & 0 & 0 & 0 & \frac{\partial h_7}{\partial \theta} & \frac{\partial h_7}{\partial m_1} & \frac{\partial h_7}{\partial m_2} & \frac{\partial h_7}{\partial I_1} & \frac{\partial h_7}{\partial I_2} & \frac{\partial h_7}{\partial \Omega_0} & \frac{\partial h_7}{\partial d_0} \\
sin(\theta) & cos(\theta) & 0 & -(1-\mu)sin(\theta) & 0 & 0 & 0 & 0 & \frac{\partial h_8}{\partial \theta} & \frac{\partial h_8}{\partial m_1} & \frac{\partial h_8}{\partial m_2} & \frac{\partial h_8}{\partial I_1} & \frac{\partial h_8}{\partial I_2} & \frac{\partial h_8}{\partial \Omega_0} & \frac{\partial h_8}{\partial d_0} \\
0 & 0 & 1 & 0 & 0 & 0 & 0 & 0 & 0 & 0 & 0 & 0 & 0 & 0 & 0 \\
-\Omega sin(\theta) & -\Omega cos(\theta) & 0 & \frac{\partial h_{10}}{\partial d} & cos(\theta) & -sin(\theta) & 0 & -(1-\mu)cos(\theta) & \frac{\partial h_1 0}{\partial \theta} & \frac{\partial h_1 0}{\partial m_1} & \frac{\partial h_1 0}{\partial m_2} & \frac{\partial h_1 0}{\partial I_1} & \frac{\partial h_1 0}{\partial I_2} & \frac{\partial h_1 0}{\partial \Omega_0} & \frac{\partial h_1 0}{\partial d_0} \\
\Omega cos(\theta) & -\Omega sin(\theta) & 0 & \frac{\partial h_{11}}{\partial d} & sin(\theta) & cos(\theta) & 0 & -(1-\mu)sin(\theta) & \frac{\partial h_1 1}{\partial \theta} & \frac{\partial h_1 1}{\partial m_1} & \frac{\partial h_1 1}{\partial m_2} & \frac{\partial h_1 1}{\partial I_1} & \frac{\partial h_1 1}{\partial I_2} & \frac{\partial h_1 1}{\partial \Omega_0} & \frac{\partial h_1 1}{\partial d_0} \\
0 & 0 & 0 & 0 & 0 & 0 & 1 & 0 & 0 & 0 & 0 & 0 & 0 & 0 & 0
\end{array}\right]
$$

Acknowledgments

An Acknowledgments section, if used, **immediately precedes** the References. Sponsorship and financial support acknowledgments should be included here. The preferred spelling of the word "acknowledgment" in American English is without the "e" after the "g." Avoid expressions such as "One of us (S.B.A.) would like to thank. . . " Instead, write "F. A. Author thanks. . . " Sponsor and financial support acknowledgments are also to be listed in the "acknowledgments" section.

References

[1] Rita K. Mann, D. J. . P. L., "FRACTION OF CONTACT BINARY TROJAN ASTEROIDS," *The Astronomical Journal*, 2007.

[2] Fujiwara, A., Kawaguchi, J., Yeomans, D. K., Abe, M., Mukai, T., Okada, T., Saito, J., Yano, H., Yoshikawa, M., Scheeres, D. J., Barnouin-Jha, O., Cheng, A. F., Demura, H., Gaskell, R. W., Ikeda, H., Kominato, T., Miyamoto, H., Nakamura, A. M., Nakamura, R., Sasaki, S., and Uesugi, K., "The rubble-pile asteroid Itokawa as observed by Hayabusa," *Science*, Vol. 312, No. 5778, 2006, pp. 1330–1334.

[3] Watanabe, S., Tsuda, Y., Yoshikawa, M., Tanaka, S., Saiki, T., and Nakazawa, S., "Hayabusa2 Mission Overview," *Space Science Reviews*, Vol. 208, 2018, pp. 3 – 16. doi:10.1007/s11214-017-0377-1.

[4] Lauretta, D. S., Bartels, A. E., Barucci, M. A., Bierhaus, E. B., Binzel, R. P., Bottke, W. F., Campins, H., Chesley, S. R., Clark, B. C., Clark, B. E., Cloutis, E. A., Connolly, H. C., Crombie, M. K., Delbó, M., Dworkin, J. P., Emery, J. P., Glavin, D. P., Hamilton, V. E., Hergenrother, C. W., Johnson, C. L., Keller, L. P., Michel, P., Nolan, M. C., Sandford, S. A., Scheeres,

D. J., Simon, A. A., Sutter, B. M., Vokrouhlický, D., and Walsh, K. J., "The OSIREX-REx target asteorid (101955) Bennu: Constraints on its physical, geological, and dynamical nature from astronomical observations," *Meteoritics & Planetary Science*, Vol. 50, 2014, pp. 834 – 849. doi:10.1111/maps.12353.

[5] Lauretta, D. S., Balram-Knutson, S. S., Beshore, E., Boynton, W. V., Drouet d'Aubigny, C., DellaGiustina, D. N., Enos, H. L., Golish, D. R., Hergenrother, C. W., Howell, E. S., Bennett, C. A., Morton, E. T., Nolan, M. C., Rizk, B., Roper, H. L., Bartels, A. E., Bos, B. J., Dworkin, J. P., Highsmith, D. E., Lorenz, D. A., Lim, L. F., Mink, R., Moreau, M. C., Nuth, J. A., Reuter, D. C., Simon, A. A., Bierhaus, E. B., Bryan, B. H., Ballouz, R., Barnouin, O. S., Binzel, R. P., Bottke, W. F., Hamilton, V. E., Walsh, K. J., Chesley, S. R., Christensen, P. R., Clark, B. E., Connolly, H. C., Crombie, M. K., Daly, M. G., Emery, J. P., McCoy, T. J., McMahon, J. W., Scheeres, D. J., Messenger, S., Nakamura-Messenger, K., Righter, K., and Sandford, S. A., "OSIRIS-REx: Sample Return from Asteroid (101955) Bennu," *Space Science Reviews*, Vol. 212, No. 1, 2017, pp. 925–984. doi:10.1007/s11214-017-0405-1.

[6] Mazanek, D. D., Merrill, R. G., Brophy, J. R., and Mueller, R. P., "Asteroid Redirect Mission concept: A bold approach for utilizing space resources," *Acta Astronautica*, Vol. 117, 2015, pp. 163–171. doi:10.1016/j.actaastro.2015.06.018.

[7] Anderson, R. C., Scheres, D., Chesley, S., and team, B., "Binary Asteroid In-Situ Explorer Mission (BASiX): A Mission Concept to Explore a Binary Near Earth Asteroid System," *45th Lunar and Planetary Science Conference, held at The Woodlands, Texas. LPI Contribution*, Vol. 1777, 2014, p. 1571.

[8] Elvis, M., "Let's mine asteroids–for science and profit: the commercial dream of trawling space for valuable minerals could bring enormous benefits to a wide range of sciences," *Nature*, Vol. 485, No. 7400, 2012, p. 549.

[9] Cheng, A. F., Rivkin, A. S., Michel, P., Atchison, J., Barnouin, O., Benner, L., Chabot, N. L., Earnst, C., Fahnestock, E. G., Kueppers, M., Pravec, P., Rainey, E., Richardson, D. C., Stickle, A. M., and Thomas, C., "AIDA DART asteroid deflection test: Planetary defense and science objectives," *Planetary and Space Science*, Vol. 157, 2018, pp. 104 – 115. doi:doi:10.1016/j.pss.2018.02.015.

[10] Rozitis, B., MacLennan, E., and Emery, J. P., "Cohesive forces prevent the rotational breakup of rubble-pile asteroid (29075) 1950 DA," *Nature*, Vol. 512, No. 7513, 2014, pp. 174–176.

[11] Hirabayashi, M., and Scheeres, D. J., "Stress and failure analysis of rapidly rotating asteroid (29075) 1950 DA," *The Astrophysical Journal Letters*, Vol. 798, No. 1, 2014, p. L8.

[12] Levy, S. D., "The Extended Kalman Filter: An Interactive Tutorial for Non-Experts," ???? URL `https://home.wlu.edu/~levys/kalman_tutorial/`, [retrieved 20 September 2018].

[13] Schneider, R., and Georgakis, C., "How to NOT Make the Extended Kalman Filter Fail," *Industrial andand Engineering Chemistry Research*, 2013, pp. 3354–3362.

[14] Luca, A. D., *Trajectory Tracking Control*, Sapienza, Universita di Roma, ????

[15] Bindu B Jagannatha, J.-B. B., and Ho, K., "Preliminary Design of Low-Energy Low-Thrust Transfers to Halo Orbits using Feedback Control," *The American Institute of Aeronautics and Astronautics Journal*, 2018.

[16] Lavretsky, E., "Adaptive Control: Introduction, Overview, and Applications," , ????

[17] John E Prussing, B. A. C., *Orbital Mechanics*, Oxford University Press, USA, 1993.

[18] Howard Kaufman, I. B., and Sobel, K., *Direct Adaptive Control Algorithms, Theory and Applications*, 2nd ed., Springer, 1998.

[19] Kumpati S. Narendra, L. S. V., "Direct and Indirect Model Reference Adaptive Control," *7th IFAC World Congress on A Link Between Science and Applications of Automatic Control*, Vol. 15, edited by Automatica, International Federation of Automatic Control, 1978, pp. 653 – 664.

[20] Koon, W. S., Lo, M. W., Marsden, J. E., and Ross, S. D., "Dynamical Systems, the Three-Body Problem and Space Mission Design," , April 2011.

[21] Szebehely, V., *Theory Of Orbits : the Restricted Problem Of Three Bodies*, Academic Press, 1967.

[22] Timm Faulwasser, P. Z., Tobias Weber, and Findeisen, R., "Implementation of Nonlinear Model Predictive Path-Following Control for an Industrial Robot," *IEEE TRANSACTIONS ON CONTROL SYSTEMS TECHNOLOGY*, Vol. 25, 2017, pp. 1505 – 1511.

[23] Eberly, D., "Distance from a Point to an Ellipse, an Ellipsoid, or a Hyperellipsoid," , ????

[24] Xiao-Diao Chen, G. W. J.-C. P. G. X., Jun-Hai Yong, "Computing the minimum distance between a point and a NURBS curve," *Elsevier, Computer-Aided Design*, Vol. 40, 2008, pp. 1051 – 1054.

[25] Eric DeJong, D. S., Scott Hudson, and Suzuki, S., "Asteroid 4179 Toutatis," Tech. rep., ???? URL `https://echo.jpl.nasa.gov/asteroids/4179_Toutatis/toutatis.html`.

[26] Jewitt, D., and Matthews, H., "Particulate Mass Loss From Comet Hale-Bopp," *The Astronomical Journal*, Vol. 117, 1999, pp. 1056 – 1062.